Supporting information

Novel Pathway of SO$_2$ Oxidation in the Atmosphere: Reactions with Monoterpene Ozonolysis Intermediates and Secondary Organic Aerosol

*Jianhuai Ye[1], Jonathan P. D. Abbatt[2], Arthur W.H. Chan[1, *]*

[1]Department of Chemical Engineering & Applied Chemistry, University of Toronto, Toronto, Canada

[2]Deparment of Chemistry, University of Toronto, Toronto, Canada

*Corresponding author (arthurwh.chan@utoronto.ca)

Supporting information summary:

Number of pages: 10
Number of figures: 7
Number of tables: 3
Number of schemes: 2

S1. SO₂ consumption in the presence of HCOOH under dry or humid conditions

B. No formic acid under dry condition
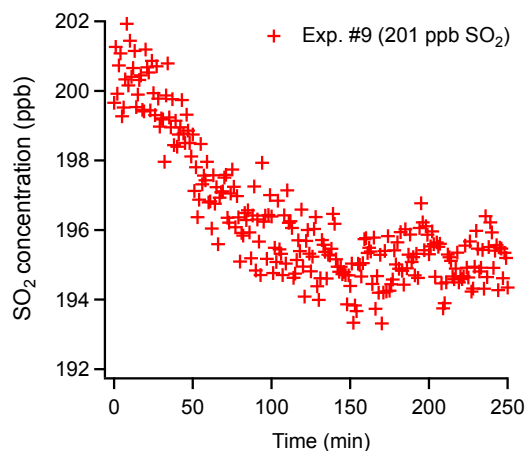
A. With formic acid under dry condition
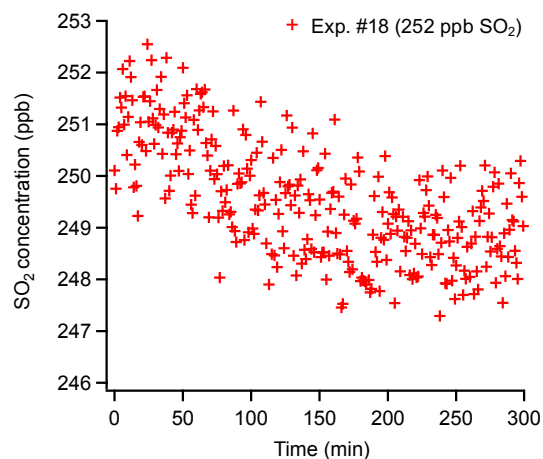
C. With formic acid under humid condition
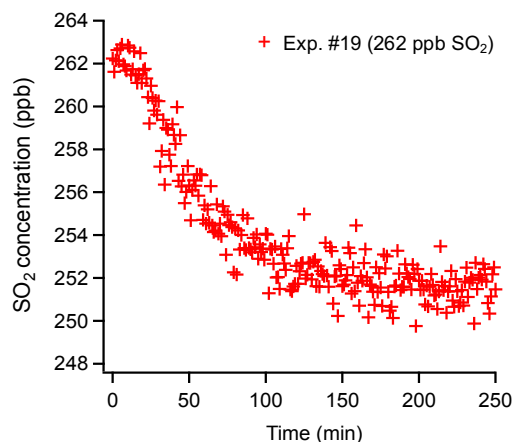
Figure S1 SO$_2$ consumption over the course of the experiments for Exp. #9 (panel A, no formic acid under dry condition), Exp. #18 (panel B, with formic acid under dry condition) and Exp. #19 (panel C, with formic acid under humid condition). By adding formic acid into SOA reaction, less SO$_2$ consumption was observed (Exp. #18 vs Exp. #9). However, as under more humid conditions, significant SO$_2$ depletion was detected even with sufficient addition of excess formic acid as Criegee Intermediate scavenger (Exp. #19 vs Exp. #9).

S2. Interactions between SO₂ and peroxides
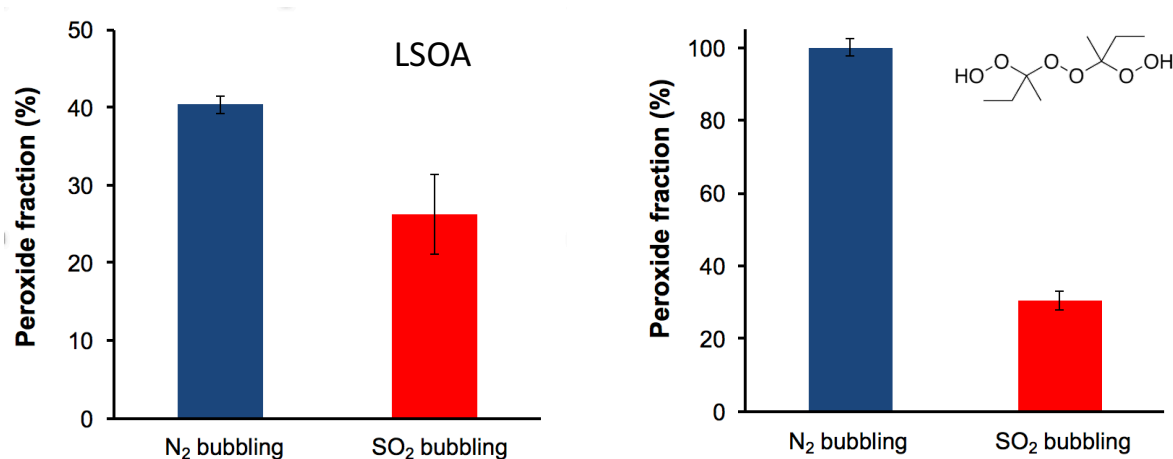
Figure S2 Peroxide fractions in SOA solution bubbled with N_2 and SO_2. Lower peroxide fraction was detected when bubbling SO_2 into LSOA solution (left panel). Significant decrease in peroxide content was also observed when bubbling SO_2 into 2-butanone peroxide solution (right panel), highlighting the importance of organic peroxide in SO_2 oxidation.

S3. SO₂ reaction with other oxidants and SO₃ experiment
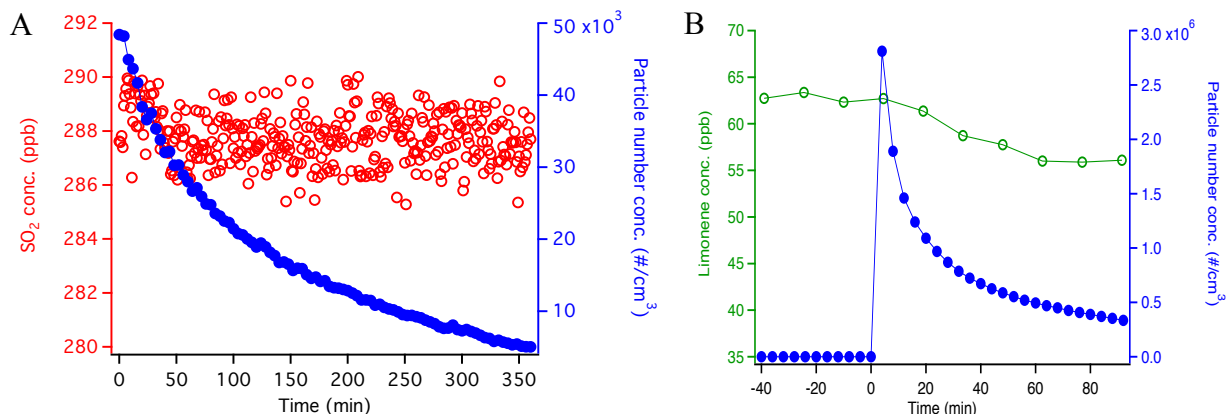
Figure S3 Two sets of control experiments to investigate other potential oxidants of SO_2. Panel A shows the change in SO_2 and particle (ammonium sulfate) concentration as a function of time in the presence of ozone (485 ppb) and formic acid (13 ppm). Panel B shows the change in limonene and particle (sulfuric acid) concentration as a function of time. It is noted that in both figures, particle concentration was not corrected for chamber wall loss.

S4. Identification of organosulfates
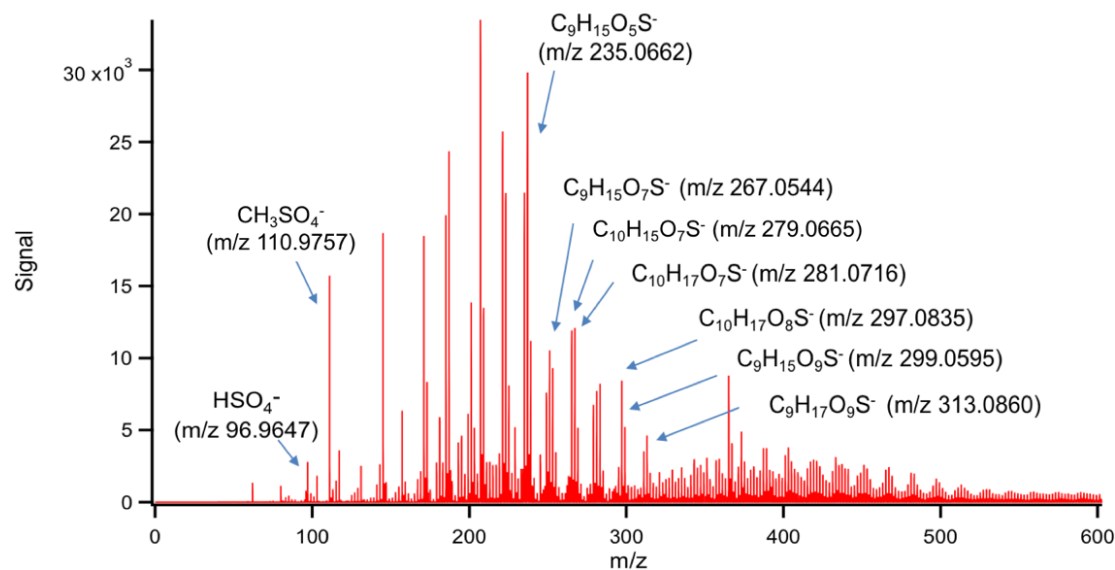
Figure S4 Organosulfates observed using ESI-IMS-TOF

Table S1 Identification of sulfur-containing ions based on IMS drift time and Kendrick mass defect

1) SO_2 : Limonene = 100 ppb : 500 ppb

Entry	[M - H]⁻	Proposed formula for [M - H]⁻	MW (M)	Identification Methods
1	96.9647	HSO_4^-	98	Mass calibration
2	110.9757	$CH_3SO_4^-$	112	IMS drift time with HSO_4^-
3	235.0662	$C_9H_{15}O_5S^-$	236	Kendrick mass defect (O) with $C_9H_{15}O_9S^-$ Kendrick mass defect (CO_2) with $C_{10}H_{15}O_7S^-$
4	267.0544	$C_9H_{15}O_7S^-$	268	Kendrick mass defect (C) with $C_{10}H_{15}O_7S^-$ Kendrick mass defect (CH_2) with $C_{10}H_{17}O_7S^-$
5	279.0665	$C_{10}H_{15}O_7S^-$	280	IMS drift time with $CH_3SO_4^-$
6	281.0716	$C_{10}H_{17}O_7S^-$	282	IMS drift time with $CH_3SO_4^-$
7	297.0835	$C_{10}H_{17}O_8S^-$	298	IMS drift time with $CH_3SO_4^-$
8	299.0595	$C_9H_{15}O_9S^-$	300	Kendrick mass defect (CH_2O) with $C_{10}H_{17}O_8S^-$ Kendrick mass defect (CH_2) with $C_{10}H_{17}O_9S^-$
9	313.0860	$C_{10}H_{17}O_9S^-$	314	IMS drift time with $CH_3SO_4^-$

2) SO_2 : Limonene = 250 ppb : 500 ppb

Entry	[M - H]$^-$	Proposed formula for [M - H]$^-$	MW (M)	Identification Methods
1	79.9573	SO_3^-	n/a	IMS drift time with HSO_4^-
2	96.9631	HSO_4^-	98	Mass calibration
3	110.9758	$CH_3SO_4^-$	112	IMS drift time with HSO_4^-
4	124.9914	$C_2H_5SO_4^-$	126	Kendrick mass defect (CH_2) with HSO_4^-, $CH_3SO_4^-$
5	179.0383	$C_6H_{11}O_4S^-$	180	Kendrick mass defect (O) with $C_6H_{11}O_8S^-$
6	186.9554	$C_2H_3O_8S^-$	188	IMS drift time with HSO_4^-
7	194.9275	$HSO_4^-(H_2SO_4)$	196	IMS drift time with HSO_4^-
8	200.9711	$C_3H_5O_8S^-$	202	IMS drift time with HSO_4^-
9	211.0282	$C_6H_{11}O_6S^-$	212	Kendrick mass defect (O) with $C_6H_{11}O_8S^-$
10	223.0282	$C_7H_{11}O_6S^-$	224	Kendrick mass defect (CH_2O) with $C_9H_{15}O_7S^-$ Kendrick mass defect (C) with $C_{12}H_{11}O_6S^-$
11	225.0438	$C_7H_{13}O_6S^-$	226	Kendrick mass defect (CH_2) with $C_6H_{11}O_6S^-$
12	229.0024	$C_5H_9O_8S^-$	230	Kendrick mass defect (CH_2) with $C_3H_5O_8S^-$
13	235.0645	$C_9H_{15}O_5S^-$	236	Kendrick mass defect (CO_2) with $C_{10}H_{15}O_7S^-$
14	239.0231	$C_7H_{11}O_7S^-$	240	Kendrick mass defect (O) with $C_9H_{15}O_7S^-$
15	243.0180	$C_6H_{11}O_8S^-$	244	IMS drift time with HSO_4^-
16	267.0544	$C_9H_{15}O_7S^-$	268	IMS drift time with HSO_4^-
17	279.0544	$C_{10}H_{15}O_7S^-$	280	IMS drift time with HSO_4^-
18	283.0307	$C_{12}H_{11}O_6S^-$	283	IMS drift time with HSO_4^-
19	299.0442	$C_9H_{15}O_9S^-$	300	Kendrick mass defect (O) with $C_9H_{15}O_7S^-$
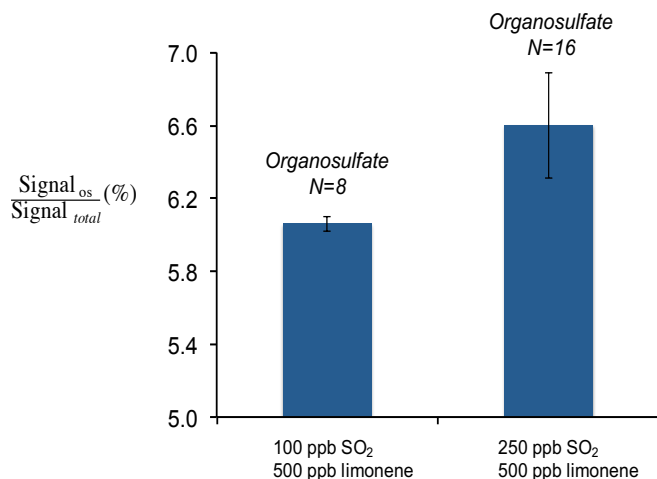
Figure S5 Fraction of total organosulfates as a function of SO_2 injection concentration during SOA formation. Both the amount and the types of organosulfates increase with increasing SO_2 concentration.

S5. α-Pinene SOA formation in the absence or presence of SO₂
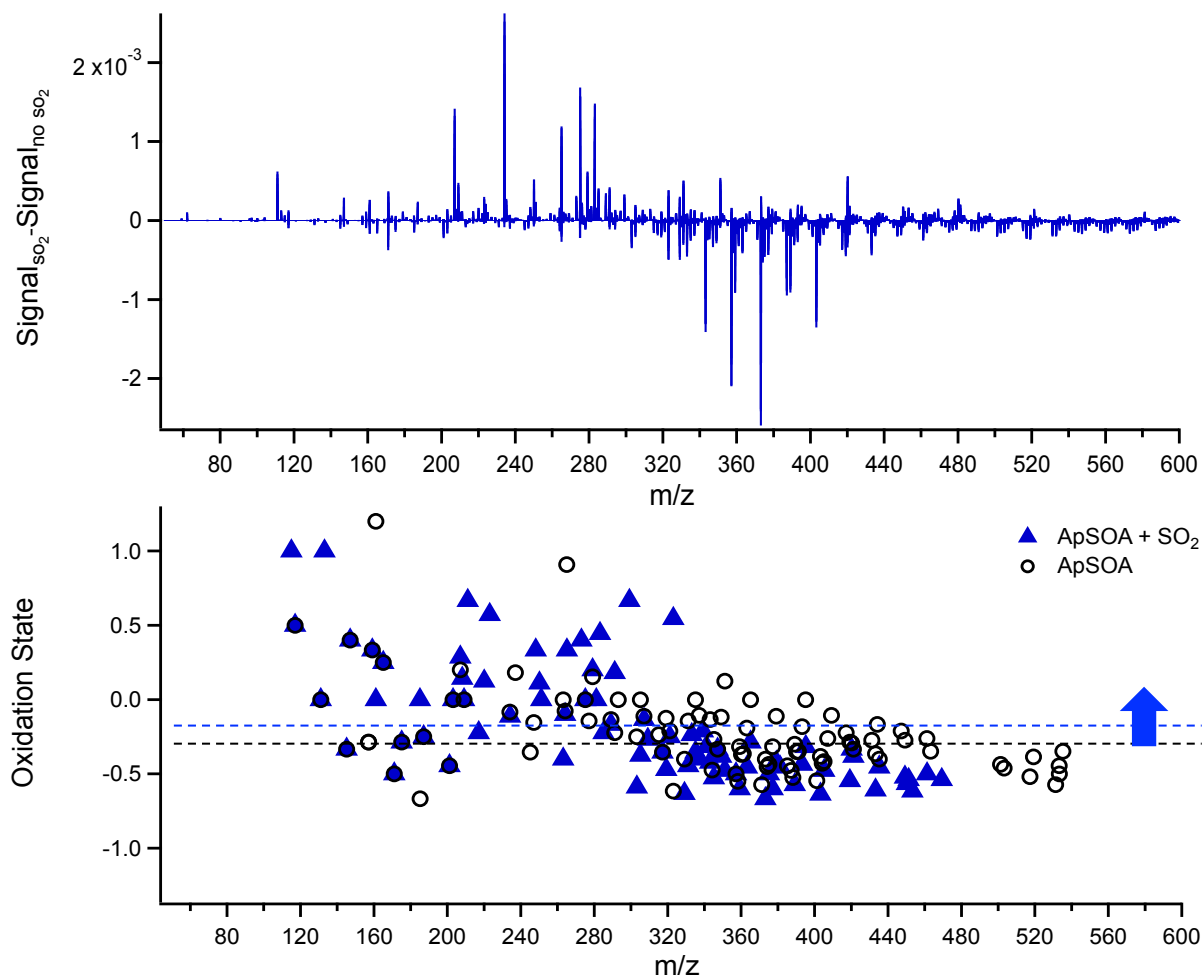
Figure S6 Difference in normalized mass spectra between ApSOA in the presence and absence of SO₂ (top panel). Signal of HSO_4^- (m/z 96.96) was not included in this comparison to investigate changes in the organic mass spectra only. Bottom panel shows the average carbon oxidation state of each peak detected in IMS-TOF and the overall average oxidation states of ApSOA (black dashed line) and ApSOA + SO₂ (blue dashed line).

S6. Gas-phase kinetic model for SO$_2$ oxidation

$$\text{Limonene} + O_3 \xrightarrow{k_1} y_{sCI}\ \text{sCI} + \text{others}$$

$$\text{Limonene} + O_3 \xrightarrow{k_2} y_{OOH}\ \text{peroxide} + \text{others}$$

$$\text{sCI} + H_2O \xrightarrow{k_3} \text{products}$$

$$\text{sCI} + (H_2O)_2 \xrightarrow{k_4} \text{products}$$

$$\text{sCI} + \text{HCOOH} \xrightarrow{k_5} \text{products}$$

$$\text{sCI} \xrightarrow{k_6} \text{products}$$

$$SO_2 + \text{sCI} \xrightarrow{k_{sCI}} \text{products}$$

$$SO_2 + \text{peroxide} \xrightarrow{k_{OOH}} \text{products}$$
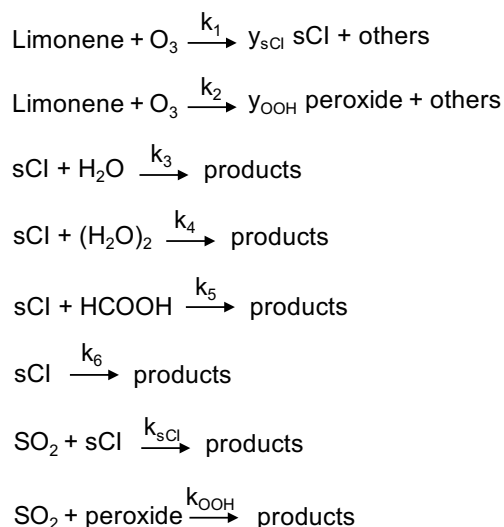
Scheme S1 Gas-phase reactions for SO$_2$ oxidation by sCI and peroxides.

Shown in Scheme S1, Criegee intermediates (sCI) and peroxides are formed from limonene ozonolysis and then react with SO$_2$.

For sCIs:

It is noted that different sCI conformers can be formed in the reaction (Scheme S2). And those conformers may have different reactivities towards reactants including water and water dimer. However, the information is lacking in the literature regarding the reactivity of limonene sCIs. To elucidate the relative importance of different pathways (sCI vs. peroxide) on SO$_2$ oxidation in our box model, reaction rate constants for sCI reactions in Scheme 1 were estimated and shown in Table S2. Two different values of k_{sCI+SO_2} were used in the simulation to examine the sensitivity of different sCI + SO$_2$ reaction rates on SO$_2$ oxidation.
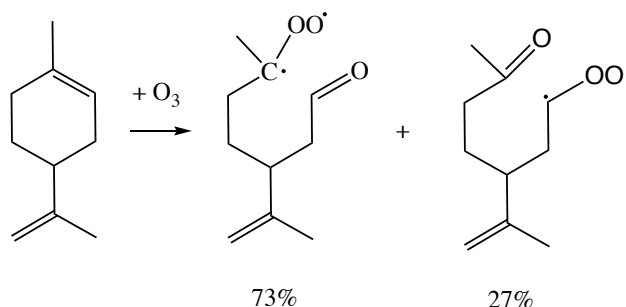
Scheme S2 Different conformers of sCIs formed from limonene ozonolysis

Table S2 Rate constants for reactions in Scheme S1

	Rate constant	**Value**	**Note**	**Literature**
k_1	$k_{\lim+O_3}$	2.1×10^{-16} cm^3 molecule^{-1} s^{-1}		(Atkinson & Arey, 2003)
k_2	k_{sCI+H_2O} (mono-substituted)	$8.8 \times 10^{-5}\, k_{sCI+SO_2}$	Estimated from k_{sCI+H_2O} of trans-2-butene	(Berndt et al., 2014)
	k_{sCI+H_2O} (di-substituted)	$4.0 \times 10^{-6}\, k_{sCI+SO_2}$	Estimated from k_{sCI+H_2O} of tetramethylethylene	(Berndt et al., 2014)
k_3	$k_{sCI+(H_2O)_2}$	$1 \times 10^3\, k_{sCI+H_2O}$		(Huang, Chao, & Lin, 2015)
k_4	$k_{sCI+formic\ acid}$	$3 \times k_{sCI+SO_2}$		(Sipilä et al., 2014)
k_5	$k_{decompose}$ (mono-substituted)	$1.2 \times 10^{12}\, k_{sCI+SO_2}$ molecule cm^{-3}	Estimated from $k_{decompose}$ of trans-2-butene	(Berndt et al., 2014)
	$k_{decompose}$ (di-substituted)	$4.2 \times 10^{12}\, k_{sCI+SO_2}$ molecule cm^{-3}	Estimated from $k_{decompose}$ of tetramethylethylene	(Berndt et al., 2014)
k_{sCI}	k_{sCI+SO_2} (high)	3.9×10^{-11} cm^3 molecule^{-1} s^{-1}	Estimated from k_{sCI+SO_2} of CH$_2$OO	(Welz et al., 2012)
	k_{sCI+SO_2} (low)	8×10^{-13} cm^3 molecule^{-1} s^{-1}	Estimated by Mauldin et al. based on field observations	(Mauldin III et al., 2012)

For peroxides:

A simplified bimolecular reaction was assumed in this study. The reaction is modelled as an irreversible pathway to match the observed SO$_2$ decay in our experiments. The simplified model is used to qualitatively demonstrate the importance of peroxide reaction pathway under our experimental conditions. It should be noted that more information about the reaction mechanisms, such as the Henry's Law constants of organic peroxides, is needed to accurately model this reaction.

The reaction rate between SO$_2$ and peroxide can be calculated as:

$$R_{SO_2+peroxide} = k_{OOH}[peroxide]\,[SO_2]$$

where k_{OOH} is the pseudo reaction rate constant (in cm^3 molecule^{-1} s^{-1}); $[peroxide]$ and $[SO_2]$ are the concentrations of peroxide and SO$_2$ (in molecule cm^{-3}), respectively.
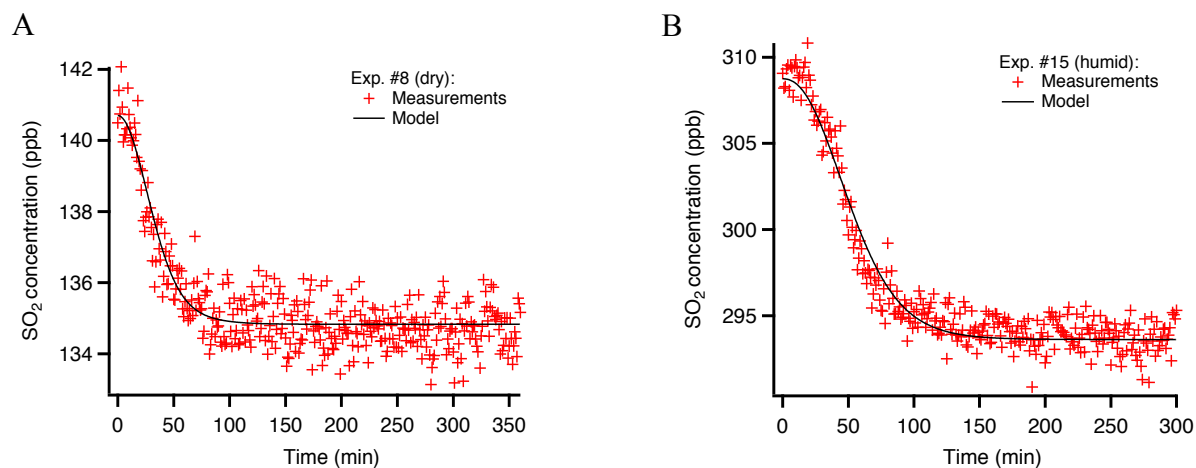
Figure S7 Examples of measured and model-simulated SO₂ concentrations under dry (A) and humid conditions (B).

Shown in Fig. 7S, the time trends of SO$_2$ in the model simulation (Scheme S1) matches those over the course of the experiments under both dry and humid conditions. Constrained from our laboratory observations, sCI yield from limonene ozonolysis (y_{sCI}) was calculated to be 0.32, which is consistent with the results from Sipilä et al. (0.27 $\pm$ 0.12) (2014). $y_{peroxide}$ that represents the available amount of peroxides in the aqueous phase that can react with SO$_2$, was calculated to be 0.06 and 0.43 under dry (10% RH) and humid (50% RH) conditions, respectively. This is likely because that under humid conditions, more aerosol water is available for peroxides to partition and to react with SO$_2$. It was also observed that k_{sCI+SO_2} did not play an important role in SO$_2$ oxidation in this simulation. Little change was observed when different reaction rates (k_{sCI+SO_2}) in Table S2 were used, indicating that the consumption of SO$_2$ was limited by the concentrations of sCIs that were available for SO$_2$ reaction.

S7. SO₂ uptake coefficient by reacting with peroxides

The uptake coefficient of SO$_2$ (γ) to the particles can be estimated using the following equation (Seinfeld & Pandis, 2006):

$$\frac{d[SO_2]}{dt} = -\frac{1}{4}\gamma A \tilde{v} [SO_2] \tag{1}$$

, where $[SO_2]$ is SO$_2$ concentration in the gas phase (molecules cm^{-3}); A is the total surface concentration of particles (m^2 m^{-3}) derived from particle size distribution measured by SMPS; $\tilde{v}$ is the mean molecular speed of SO$_2$ (m s^{-1}) which is obtained from:

$$\tilde{v} = \sqrt{\frac{8RT}{MW\pi}} \tag{2}$$

, where R is the gas constant; T is the experiment temperature; MW is the molecular weight of SO$_2$.

To calculate the uptake coefficient, we assume the fraction of SO$_2$ that reacted with peroxides ($f_{(SO_2+peroxide)}$) was constant over the course of the experiment, Eq. (1) can be then modified as:

$$ln\frac{[SO_2]_0}{[SO_2]_t} = \ln\frac{[SO_2]_0}{[SO_2]_0 -([SO_2]_0-[SO_2]_t)f_{(SO_2+peroxide)}} = \frac{1}{4}\gamma A\tilde{v}\,\Delta t \qquad (3)$$

where $[SO_2]_0$ and $[SO_2]_t$ are SO$_2$ concentration at 0 min and t min, respectively; Since SO$_2$ consumption ceased when t is around 150 min for all the limonene experiments under humid conditions, $\Delta t = 150$ min was used in all the calculations. We therefore present a conservative estimate of SO$_2$ uptake coefficients, shown in Table S3.

Table S3 Estimated uptake coefficients of SO$_2$ through reacting with peroxides from limonene ozonolysis under humid conditions

Exp. #	$[SO_2]_{0\,min}$ (ppb)	$[SO_2]_{150\,min}$ (ppb)	S (m^2 m^{-3}) [a]	$f_{(SO_2+peroxide)}$ [b]	RH (%)	γ
14	144.3	128.9	2.24×10^{-3}	0.84	55%	5.1×10^{-5}
15	308.8	293.8	2.32×10^{-3}	0.76	47%	1.8×10^{-5}
19	262.2	252.2	1.73×10^{-3}	0.77	50%	1.9×10^{-5}
20	605.4	593.0	1.57×10^{-3}	0.75	52%	1.1×10^{-5}

[a]: average total particle surface area concentration in the first 150 min of the experiments;
[b]: the fraction of SO$_2$ that reacted with peroxides, calculated using the modeling simulation results from Section S6

Reference

Atkinson, R., & Arey, J. (2003). Atmospheric degradation of volatile organic compounds. *Chemical Reviews*, *103*(12), 4605–4638. https://doi.org/10.1021/cr0206420

Berndt, T., Jokinen, T., Sipilä, M., Mauldin, R. L., Herrmann, H., Stratmann, F., … Kulmala, M. (2014). H$_2$SO$_4$ formation from the gas-phase reaction of stabilized Criegee Intermediates with SO$_2$: Influence of water vapour content and temperature. *Atmospheric Environment*, *89*, 603–612. https://doi.org/10.1016/j.atmosenv.2014.02.062

Huang, H.-L., Chao, W., & Lin, J. J.-M. (2015). Kinetics of a Criegee intermediate that would survive high humidity and may oxidize atmospheric SO$_2$. *Proceedings of the National Academy of Sciences*, *112*(35), 10857–10862. https://doi.org/10.1073/pnas.1513149112

Mauldin III, R. L., Berndt, T., Sipilä, M., Paasonen, P., Petäjä, T., Kim, S., … Kulmala, M. (2012). A new atmospherically relevant oxidant of sulphur dioxide. *Nature*, *488*(7410), 193–196. https://doi.org/10.1038/nature11278

Seinfeld, J. H., & Pandis, S. N. (2006). *Atmospheric chemistry and physics: from air pollution to climate change. Atmospheric Chemistry and Physics* (2nd Ed.). Wiley: New York.

Sipilä, M., Jokinen, T., Berndt, T., Richters, S., Makkonen, R., Donahue, N. M., … Petäjä, T.

(2014). Reactivity of stabilized Criegee intermediates (sCIs) from isoprene and monoterpene ozonolysis toward SO_2 and organic acids. *Atmospheric Chemistry and Physics*, *14*(22), 12143–12153. https://doi.org/10.5194/acp-14-12143-2014

Welz, O., Savee, J. D., Osborn, D. L., Vasu, S. S., Percival, C. J., Shallcross, D. E., & Taatjes, C. A. (2012). Direct kinetic measurements of Criegee intermediate (CH_2OO) formed by reaction of CH_2I with O_2. *Science*, *335*(6065), 204–207. https://doi.org/10.1126/science.1213229